



An application of deep learning technique to improve S2S Rainfall Forecast over Java Island, Indonesia

Adyaksa Budi Raharja^{ab}, Akhmad Faqih^b, Amsari Mudzakir Setiawan^a

^a Center for Climate Change Information, Meteorological Climatological and Geophysical Agency (BMKG), Kemayoran, Central Jakarta, 10610, Indonesia

^b Department of Geophysics and Meteorology, Faculty of Mathematics and Natural Sciences, IPB University, IPB Dramaga Campus, Bogor, 16680, Indonesia

Article Info:

Received: 13 - 01 - 2022

Accepted: 12 - 08 - 2022

Keywords:

Bias correction, convolutional autoencoders, rainfall forecasts, sub-seasonal to seasonal

Corresponding Author:

Akhmad Faqih

Department of Geophysics and Meteorology, Faculty of Mathematics and Natural Sciences, IPB University;

Email:

akhmadfa@apps.ipb.ac.id

Abstract. *Subseasonal to seasonal (S2S) rainfall forecast can benefit several sectors, such as water resources, hazard management, and agriculture. However, the forecast remains challenging due to its lack of skill. This study applies Convolutional AutoEncoders (ConvAE), a deep learning technique, to improve the quality of the S2S rainfall forecast. Seven S2S model outputs incorporated with Subseasonal Experiments Projects (SubX), including CCSM4, CFSv2, FIMr1p1, GEFS, GEOS_v2p1, GEPS6, and NESM, are corrected using the ConvAE approach. We combine 407 ground observations and the CHIRPS dataset using regression kriging methods producing gridded daily precipitation data with 0,05° spatial resolution. We utilize this dataset as a label to train ConvAE models and to perform bias corrections to all members of the SubX forecast data. The results show that ConvAE is able to increase the quality of weekly S2S rainfall forecasts over Java, Indonesia. The Correlation Coefficient for 1–4 weeks lead time are improved from: 0,76; 0,715; 0,692 and 0,722 towards 0,809; 0,751; 0,719 and 0,74; respectively. Furthermore, the average CRPSS improves between 20-30% for all lead times.*

How to cite (CSE Style 8th Edition):

Raharja AB, Faqih A, Setiawan AM. 2022. An application of deep learning technique to improve S2S Rainfall Forecast over Java Island, Indonesia. *JPSL* 12(4): 587–598. <http://dx.doi.org/10.29244/jpsl.12.4.587-598>.

INTRODUCTION

Subseasonal to Seasonal forecasting (S2S) is a forecast that scales around two weeks to a season in advance, bridging weather and climate forecasting (Robertson and Vitart 2019). S2S was recognized as a challenging time scale compared to other time scales and is often known as a “desert of predictability” due to its lack of skill (Vitart *et al.* 2017). However, its advantages to several sectors, such as public health, humanitarian, energy, water resource, hazard management, and agricultural field, lead to increasing demand for forecasts at this time scale (White *et al.* 2017; Vuillaume *et al.* 2018). Therefore, the operational, scientific, and application communities are becoming increasingly interested in developing (Robertson *et al.* 2015) and improving the quality of S2S forecasts (Kolachian and Saghafian 2019; Li *et al.* 2019; Wang *et al.* 2021).

There are at least two approaches that can be used to improve the skills of S2S climate forecasting. The first approach is improving the quality of the dynamic climate model or the Earth system model itself, and the second one is postprocessing the climate model's output (Baker *et al.* 2020). Statistical postprocessing is aimed at correcting the biases and dispersion errors of the dynamic forecast model output. Its methods span from traditional bias correction to more sophisticated methods (Ratri *et al.* 2019), including machine learning.

Recently, machine learning has received renewed attention in various fields over the last decade, owing to significant breakthroughs made with Deep Learning (DL) models. Because of its (deep) layered structure, DL can hierarchically extract high-level feature illustrations. Convolutional Neural Network (CNN) has gotten much attention in spatiotemporal data sets because of their ability to learn spatial pattern from data (Baño-Medina *et al.* 2020). Han *et al.* (2021) implemented CU-net, a CNN-based deep learning technique, in order to bias correct ECMWF 1-10 days forecasts. The results show an improvement in bias correction, coefficient correlation, root mean squared error and Mean Absolute Error (MAE).

Le *et al.* (2020) corrected the grid-by-grid bias in satellite precipitation estimates using the Convolutional autoencoder (ConvAE), a CNN-based bias correction approach. The ConvAE model, according to Le *et al.* (2020), performed admirably in capturing spatial patterns, trends, and extremes. It proves the ability of the ConvAE model to bias correct satellite precipitation data. The same approach but with a different architecture was used to develop a Statistical Downscaling Model (SDM) for precipitation estimates over Northern Africa, demonstrating excellent reproducibility of the temporal rainfall projections (Babaousmail *et al.* 2021). To our knowledge, CNN has never been applied in correcting S2S forecasts in Indonesia. Nevertheless, a comparable method, one-dimensional CNN, has been used to predict the air temperature in Padang and produce satisfying results compared to Multilayer Perceptron (MLP) (Kurniawan *et al.* 2020).

Despite error and dispersion problems, the dynamic forecast model output will always exhibit uncertainty problems (Muharsyah *et al.* 2020). One source of this uncertainty is the limited information regarding the initial conditions of the climate system (Monier *et al.* 2015). However, this problem can be addressed using an ensemble prediction system or Multimodel Ensemble (MME) approach (Krasnopolsky and Lin 2012).

This study aims to improve the quality of S2S rainfall prediction by applying ConvAE, a CNN-based bias correction technique, and employing MME in its corrected forecasts. We train historical S2S forecast data from The Subseasonal Experiment Projects (SubX) using gridded precipitation data that we produced using multiple linear regression residual kriging to develop a ConvAE trained model. Furthermore, we use the ConvAE trained model to bias correct the SubX S2S forecasts and acquire improved S2S forecasts. After that, we performed the evaluation using RMSE and Correlation Coefficient, also Continuous Ranked Probabilistic Skill Score (CRPSS) for deterministic and probabilistic forecasts, respectively. The evaluation was performed for every single model and multimodel ensemble on a weekly time scale.

METHODOLOGY

Data

Combined satellite and ground observation with spatial resolution $0,05^\circ \times 0,05^\circ$ at daily time scales have been used in this study. Following Misnawati *et al.* (2018), we combine 378 ground observations obtained from BMKG (find blue dots in Figure 1) and CHIRPS satellite estimation products (Funk *et al.* 2015) using multiple linear regression and residual kriging, while 99 stations (find black dots in Figure 1) have been used to evaluate this method. This approach has been exposed to perform well in correcting CHIRPS data over Java and introducing the best agreement to the ground observation data (Misnawati *et al.* 2018). This combined dataset was then used as a label in the deep learning technique to correct S2S forecasts in the next stage.

This study also utilized seven S2S model outputs incorporated with Subseasonal Experiment Projects (SubX) consisting of CCSM4, CFSv2, FIMr1p1, GEFS GEOS_v2p1, GEPS6, and NESM. The SubX model covers the global domain at 1° x 1° spatial resolution and the daily time scale with ±18 years of hindcasts data and ±18 months of real-time forecasts (Pegion *et al.* 2019). This dataset was made publicly available through the IRI Data Library and might be accessed via the following link: <https://iridl.ldeo.columbia.edu/SOURCES/.Models/.SubX/>. More detailed information regarding the model’s institution, ensemble member, update interval, lead time, and time-coverage of hindcasts and forecasts of the utilized SubX data (Kirtman *et al.* 2017) can be found in Table 1.

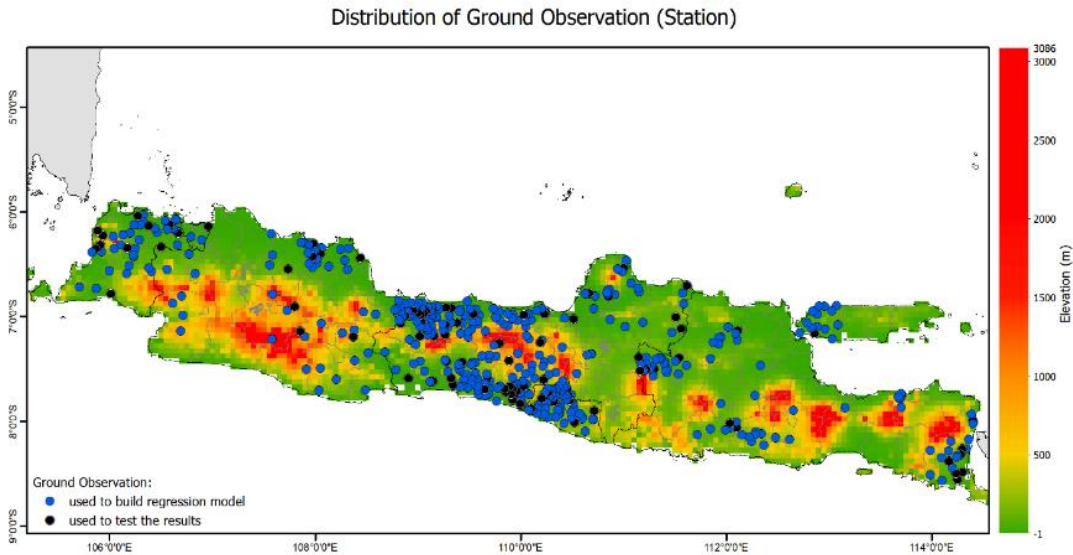


Figure 1 The topography of Java Island and the distribution of ground observation

Table 1 SubX model data was used in this study

Institution Models	Lead time (days)	Hindcasts			Forecasts		
		Ens-Member (per day)	Init-interval (days)	Time coverage	Ens-Member (per day)	Init-update	Start dates
RSMAS-CCSM4	45	3	7	1999 - 2016	9	Sunday	12/31/2017 – 12/29/2019
NCEP-CFSv2	44	4*	1	1999 - 2016	4	Everyday	12/31/2017 – 12/31/2019
ESRL-FIMr1p1	32	5	7	1999 - 2016	4	Wednesday	12/27/2017 – 12/25/2019
EMC-GEFS	35	11	7	1999 - 2016	21	Wednesday	12/27/2017 – 12/25/2019
ECCC-GEPS6	32	4	7	1999 - 2016	21	Thursday	12/28/2017 – 12/26/2019
GMAO-GEOS_v2p1	45	4	5	1999 - 2016	4	rotates	12/27/2017 – 12/27/2019
NRL-NESM	45	1	4-every weeks	1999 - 2016	1**	Saturday-Tuesday	12/30/2017 – 12/31/2019

Note: *initialized four times a day, but we only used the data that initialized at 00:00Z; ** updated four times a week. Therefore, we used all init-update

From Table 1, we noticed that each model have different ensemble member, interval, and start dates in the hindcast and forecast period. Therefore, we used the model ensemble mean in the hindcast period and averaged it to all start dates available for the following training process described in Figure 2. Furthermore, we choose the latest issues closest to the 1-4 weeks target forecasts to handle the different forecast start dates. All SubX data were then re-gridded to $0,05^{\circ}$ applying bilinear interpolation to match the spatial resolution of the observation dataset. This re-gridded dataset was then fed to the deep-learning models in the next step.

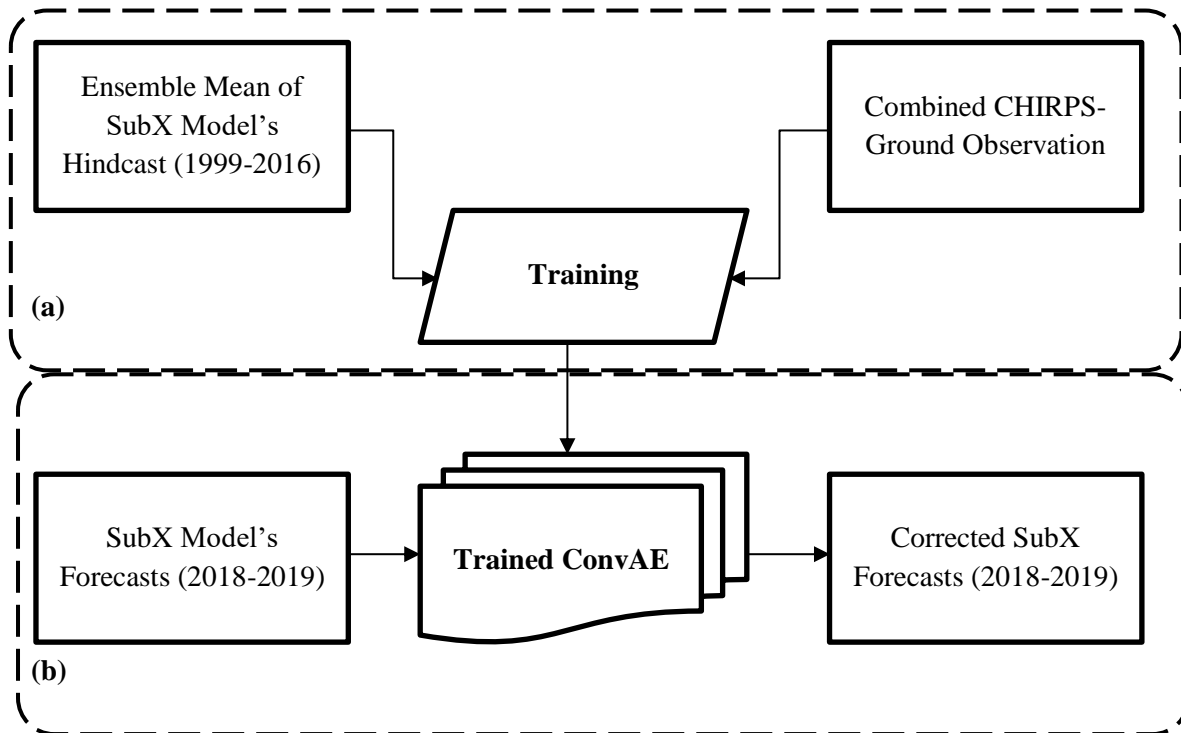


Figure 2 ConvAE flowchart: (a) Model training, (b) Model application

Convolutional Auto Encoders (ConvAE)

This study applied the ConvAE architecture to correct the bias of SubX model output. ConvAE merges the architecture of CNN with autoencoder (AE), which consists of an encoder and decoder. Encoders employ an effective learning process in compressing and encoding data by reducing data dimensions and letting the noise pass through while the decoder reconstructs the encoded data as similar as possible to the input data (Le *et al.* 2020). ConvAE is commonly used in image noise reduction, hence it could also be applied in statistical downscaling or bias correction.

Initially, we train the ensemble mean of hindcast data from seven SubX models using ConvAE separately. In the training process, we split the hindcast data from 1999-2016 into proportion 2:1 as training and validation sets, respectively. The ConvAE training has been carried out with 100 epochs, a filter size of 3 x 3 kernels, and a batch size of 32. The reluactivation function was applied in all convolution layers, while the linear activation function has applied in the MaxPooling and Upsampling layers. The MSE loss function with a learning rate of 0,00001 and Adam function as an optimizer was used to train the model. Table 2 explains the detailed architecture of ConvAE used in this study.

The training processes were resulting seven trained ConvAE models. These trained ConvAE models were then used to correct the raw SubX model's output. We have conducted the bias correction to all members of the SubX model's output (67 members in total) at daily time scales for 2018-2019. The general process of the deep learning technique that has been applied is described in Figure 2.

Table 2 Detailed architecture of ConvAE used in this study

Layer (type)	Output Shape	Parameter #	Connected to
input 1 (InputLayer)	(None, 224, 224, 1)		
conv2d 37 (Conv 2D)	(None, 224, 224, 5)	50	input 1 [0] [0]
max pooling 2d 37 (MaxPooling2D)	(None, 112, 112, 5)	0	conv2d 37 [0] [0]
conv2d 38 (Conv2D)	(None, 112, 112, 10)	460	max pooling2d 17[0] [0]
max pooling 2d 38 (MaxPooling2D)	(None, 56, 56, 10)	0	conv2d 38 [0] [0]
conv2d 39 (Conv2D)	(None, 56, 56, 15)	1.365	max pooling2d 38 [0] [0]
max pooling 2d 39 (MaxPooling2D)	(None, 28, 28, 15)	0	conv2d 39 [0] [0]
conv2d 40 (Conv2D)	(None, 28, 28, 20)	2.720	max pooling2d 39 [0] [0]
max pooling 2d 40 (MaxPooling2D)	(None, 14, 14, 20)	0	conv2d 40 [0] [0]
conv2d 41 (Conv2D)	(None, 14, 14, 25)	4.525	max pooling2d 40 [0] [0]
conv2d 42 (Conv2D)	(None, 14, 14, 128)	28.928	conv2d 41 [0] [0]
up sampling 2d 42 (UpSampling2D)	(None, 28, 28, 128)	0	conv2d 42 [0] [0]
conv2d 43 (Conv2D)	(None, 28, 28, 128)	147.584	up sampling2d 42 [0] [0]
up sampling 2d 43 (UpSampling2D)	(None, 56, 56, 128)	0	conv2d 43 [0] [0]
conv2d 44 (Conv2D)	(None, 56, 56, 128)	147.584	up sampling2d 43 [0] [0]
up sampling 2d 44 (UpSampling2D)	(None, 112, 112, 128)	0	conv2d 44 [0] [0]
conv2d 45 (Conv2D)	(None, 112, 112, 128)	147.584	up sampling2d 44 [0] [0]
up sampling 2d 45 (UpSampling2D)	(None, 224, 224, 128)	0	conv2d 45 [0] [0]
conv2d 46 (Conv2D)	(None, 224, 224, 1)	1.153	up sampling2d 45 [0] [0]
add (Add)	(None, 224, 224, 1)	0	conv2d 46 [0] [0] input 1 [0] [0]

Note: Total parameters: 481.953; Trainable parameters: 481.953; Non-trainable parameters: 0.

Performance Evaluation

The performance evaluation has been conducted to the raw and ConvAE corrected for lead 1–4 weeks forecasts. In this study, we evaluated the multimodel ensemble mean forecasts using coefficient correlation (CC) and RMSE. Furthermore, probabilistic forecasts were assessed using Continuous-Ranked Probabilistic Skill Score (CRPSS). These indicators were calculated grid-by-grid of raw and ConvAE corrected forecasts at a weekly time scale.

Root Mean Square Error (RMSE)

RMSE was calculated to assess deterministic forecast performances. RMSE measured the differences between the prediction of a model as an estimate of the observed values. The formulation of RMSE is defined as follows:

$$RMSE = \sqrt{\frac{1}{n} \sum_{i=1}^n (o_i - f_i)^2}$$

Here o_i denotes the observed weekly precipitation records, and f_i denotes the weekly precipitation forecasts. The RMSE values displayed in Figure 3 were calculated over 2018-2019 and averaged over all periods.

Correlation Coefficients (CC)

The correlation coefficient (r) between forecasts and observed weekly rainfall was also used for measuring model performance and defined as follows:

$$r = \frac{\sum_i^n (f_i - \bar{f})(o_i - \bar{o})}{\sqrt{\sum_i^n (f_i - \bar{f})^2} \sqrt{\sum_i^n (o_i - \bar{o})^2}}$$

where \bar{o} and \bar{f} denotes the average of observed and forecasts weekly precipitation, respectively.

Continuous-Ranked Probabilistic Skill Score (CRPSS)

CRPSS measured skills of the probabilistic prediction relative to the forecast reference. CRPSS compares CRPS from the predicted rainfall (raw or corrected) against the climatological mean prediction reference. CRPS can be formulated as follows (Ratri *et al.* 2019):

$$CRPS = \int_{-\infty}^{\infty} [F(fcst) - F_o(fcst)]^2$$

where $F(fcst)$ is the CDF of the predicted ensemble and $F_o(fcst)$ is a Heaviside function that has a value of 0 if the forecasts value < observed value and a value of 1 if the forecasts value \geq observed value. CRPSS can be defined as follows:

$$CRPSS = 1 - \frac{CRPS_{fcst}}{CRPS_{ref}}$$

where $CRPS_{fcst}$ is the ensemble forecast CRPS, while $CRPS_{ref}$ is the reference (climatological) forecast CRPS. The CRPSS value spans from $-\infty$ to 1. A positive result implies that the prediction outperforms the prediction reference; 1 is the perfect score of CRPSS.

RESULT AND DISCUSSION

Area Averaged Forecasts

Figures 3 and 4 illustrate the weekly area-averaged rainfall forecasts of seven raw and ConvAE corrected the SubX model's output for lead time 1–4 weeks, respectively. The thick black and blue lines indicate observation and SubX MME, while other colors indicate the ensemble mean of seven single models incorporated in SubX. Moreover, the blue shades in these figures explain the spreads of all 67 SubX's ensemble members.

Figure 3 shows that all raw models in all lead times have better represented the actual observation at the dry season (Jul–Oct), indicated by all model lines that almost coincide with the observation. Nevertheless, almost all models have shown a large gap with the observation at the wet season (Dec–Mar). Regarding lead time, Figure 3 shows a slightly decreasing predictive quality as the increase of lead time forecasts, especially during the wet season. Related to Figure 3, Figure 4 shows an improvement in prediction quality compared to the raw ones. The gap between SubX MME and observation is narrowing in all lead times and all models. Besides, the ensemble spread of the ConvAE corrected forecast was also smaller compared to the raw forecast. It theoretically indicates higher forecast accuracy since it has smaller uncertainty (Barker 1991).

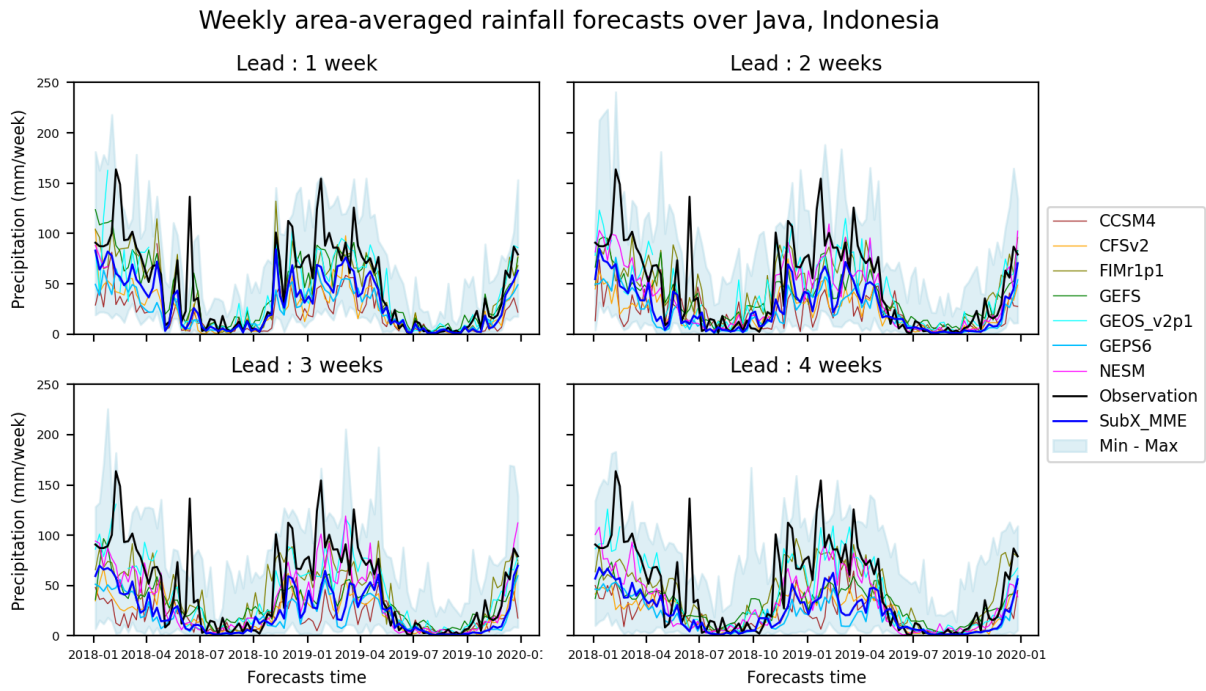


Figure 3 Weekly area-averaged rainfall forecasts of the raw SubX model's output over Java, Indonesia for lead time 1–4 weeks in 2018–2019

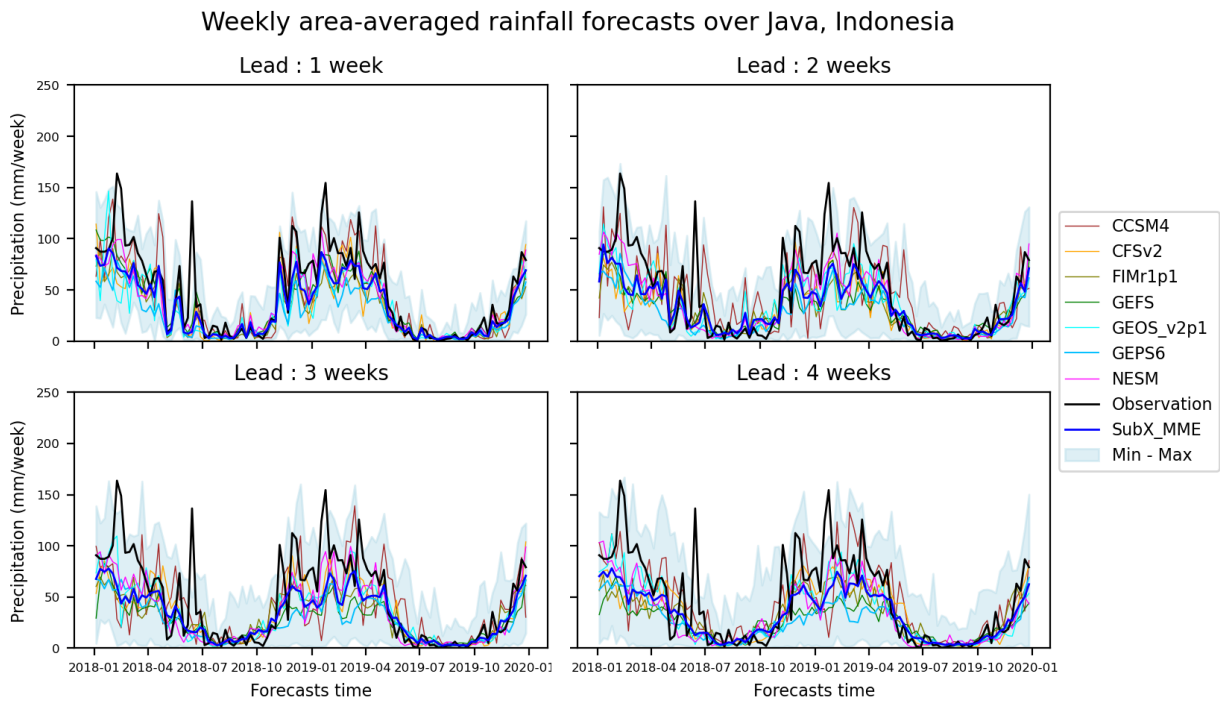


Figure 4 Weekly area-averaged ConvAE corrected rainfall forecasts over Java, Indonesia for lead time 1–4 weeks in 2018–2019

Correlation Coefficient (CC)

CC assesses the linear relationship between weekly observed and rainfall forecast for all grid points in the 2018–2019 periods. Figure 5 clarifies CC improvement of ConvAE corrected forecasts compared to SubX raw forecasts at weekly time scales, except for three weeks lead time. The CC for lead 1,2 and 4 weeks

improved from: 0,787; 0,753; and 0,746 towards 0,824; 0,768; and 0,757; respectively. Spatially, CC for all lead times was ranged from 0,7-0,8 for most areas of Java Island, except the western part of Java (Banten Province) and the North-Eastern part of Central Java which has a value up to 0,6.

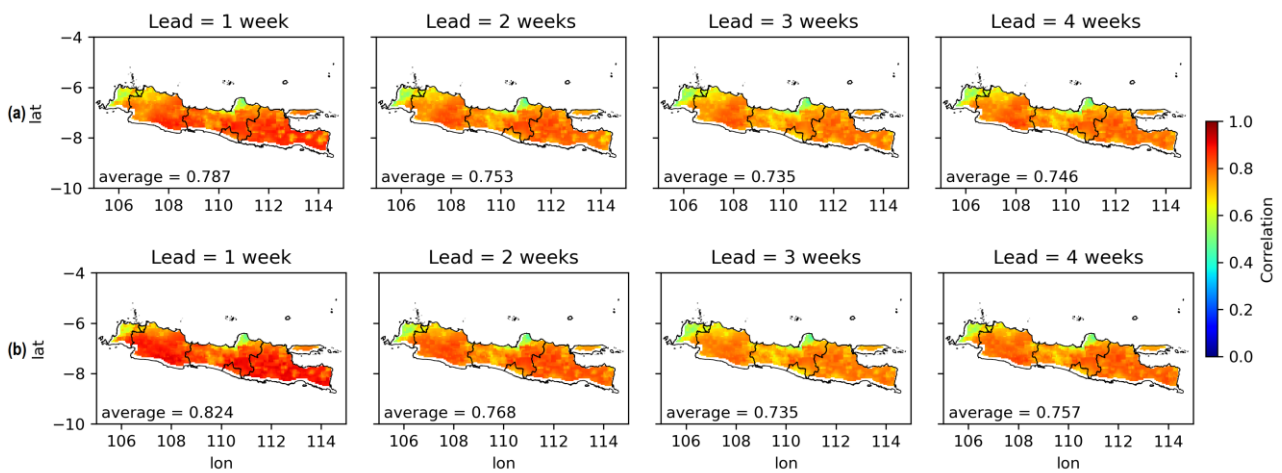


Figure 5 The correlation coefficient between SubX MME weekly rainfall forecasts and observation of (a) raw and (b) ConvAE corrected for lead time 1–4 weeks

Root Mean Square Error (RMSE)

RMSE was calculated for raw, and ConvAE corrected SubX MME weekly rainfall forecasts over Java, Indonesia for 2018–2019. The results show that averaged RMSE values were slightly decreased for all leads in ConvAE corrected forecasts. Generally, the eastern part of Java has a lower RMSE value compared to other areas. It could be clearly shown in one week lead time, while the eastern part of Java mostly has RMSE values up to 25 in ConvAE corrected forecasts, except for the mountainous areas with RMSE values >50. The center and western part of Java commonly shows RMSE values >30 in one week lead time.

Continuous-Rank Probability Skill Score (CRPSS)

Figure 7 shows that ConvAE typically improves CRPSS values up to 0.5 in the one week lead time. The area-averaged of CRPSS improves from 0,294; 0,205; 0,176 and 0,167 towards 0,384; 0,254; 0,211 and 0,218; for week 1–4 forecasts, respectively. Their improvement varies between 20–30%, with the greatest improvement occurring in one week lead time. The highest CRPSS score also happened in the one-week lead time. At the same time, the lowest appeared in the four-week lead time of raw SubX MME forecast. Related to the spatial pattern of RMSE values in Figure 6, the CRPSS of the eastern part of Java also introduced better values compared to the western part of Java. It could be because eastern Java’s dry season is more steadily dry than the western part, and Java’s western part experiences greater rainfall variability (Ratri *et al.* 2019).

If we take a closer look at Figure 6, Figure 7 and compare them to Figure 1, we can conclude that higher RMSE values and lower CRPSS scores are associated with local topographic effects. Since the higher RMSE values and lower CRPSS values are persistent occurred in the mountainous area. The poor skill at mountainous areas in raw models might be due to coarse spatial resolution of GCM output that do not incorporate local topographic effect (Nover *et al.* 2016). The primary and most persistent circulation error in global NWP and GCM is an insufficient depiction of orographic influence on atmospheric flow (Sandu *et al.* 2019). The ConvAE could not address this problem since the RMSE values are still high and CRPSS values remain low in the mountainous area. It could be affected by the deep network in our ConvAE architecture that usually discards detailed image information, presumably because too much detail is already lost during convolution and pooling (Mao *et al.* 2016).

Figure 8 shows averaged RMSE, correlation coefficient, and CRPSS for all individual models compared to SubX MME. The upper row is all raw model forecasts, while the bottom row is ConvAE corrected forecasts. In general, the area-averaged RMSE values of ConvAE corrected forecasts are decreased compared to raw ones, except for GEFS, which increased for 2–4 weeks lead times. Depending on models and lead times, the improvement of RMSE values varies up to 39%. Furthermore, the most remarkable RMSE improvements occurred in NESM for one week lead time, which improved from 47,2 to 28,8. A further area-averaged correlation coefficient is increased between 0,006-0,201, which one week lead time of NESM also recording the notable increases. It also happened in CRPSS, while the CRPSS value of NESM in one week lead time was improved from -0,437 to 0,327. Another notable enhancement occurred in CCSM4 at one and four weeks lead time and CFSv2 at all lead times, where CRPSS improved from negative to positive after ConvAE bias correction.

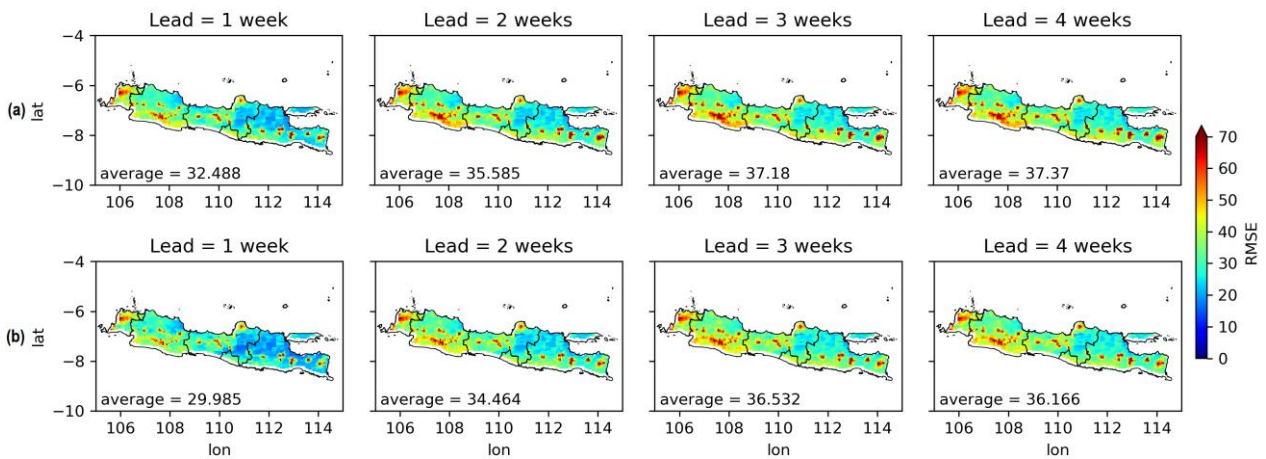


Figure 6 RMSE of (a) raw and (b) ConvAE corrected SubX MME weekly rainfall forecasts for lead time 1-4 weeks

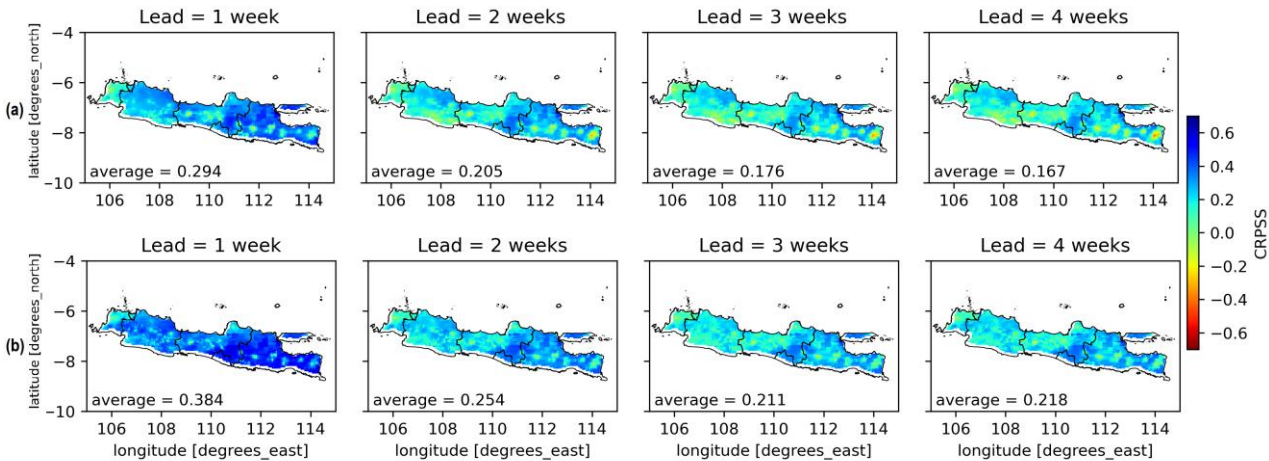


Figure 7 Overall CRPSS of (a) raw and (b) ConvAE corrected SubX MME weekly rainfall forecasts for lead time 1–4 weeks

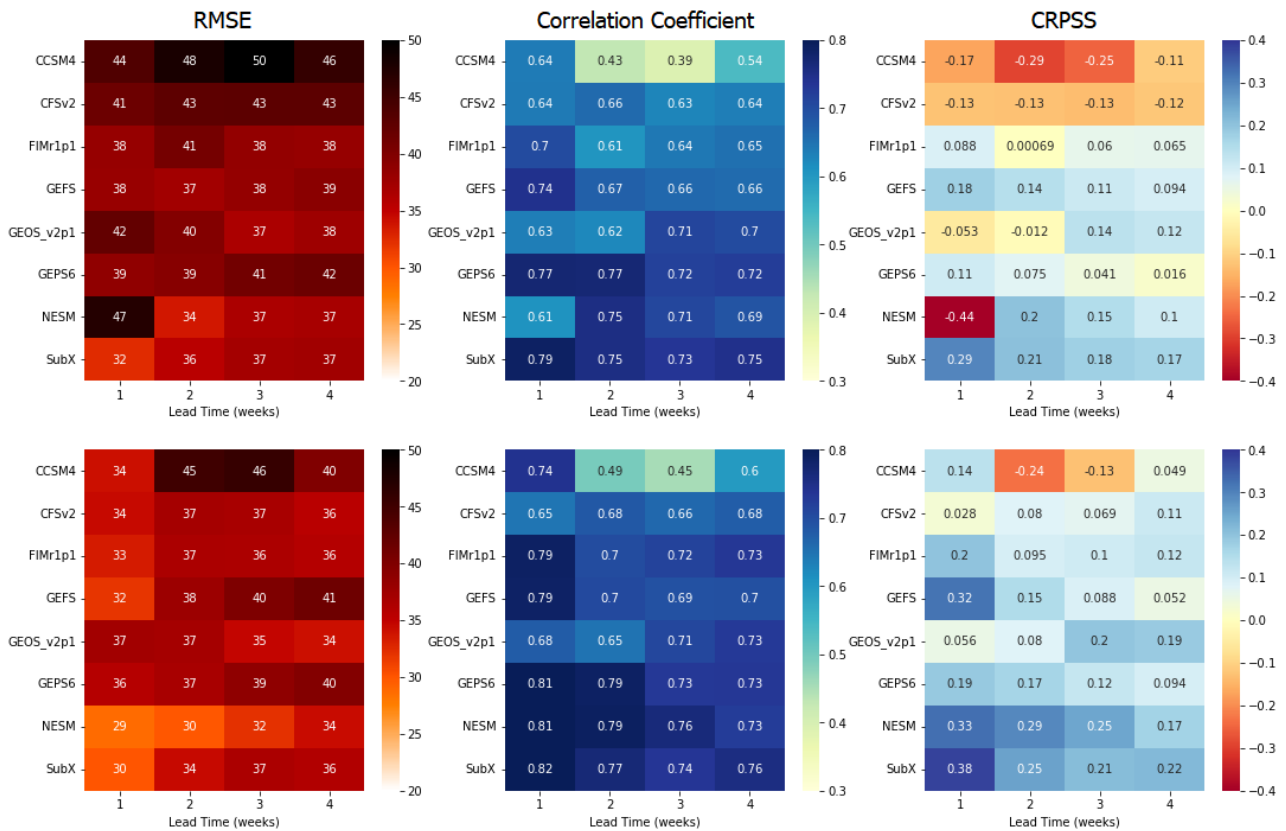


Figure 8 Area averaged weekly rainfall forecasts skill (RMSE, Correlation Coefficient and CRPSS) of raw (upper) and ConvAE corrected (lower) SubX models for lead time 1–4 weeks

CONCLUSIONS

This study has implemented convolutional autoencoders (ConvAE), a deep learning technique, to improve S2S rainfall forecasts over Java, Indonesia. The results show that ConvAE has increased the quality of weekly S2S rainfall forecasts over Java, Indonesia, by improving the correlation coefficient and CRPSS and decreasing the RMSE value. Although we have demonstrated that the ConvAE could effectively improve the prediction skills of weekly forecasts in general, the ConvAE could not address poor skills in the mountainous area. It might result from the deep ConvAE network architecture that usually ignores detailed image information because too much detail is already lost during the convolution and pooling process. We suggest employing a skip connection, e.g., U-NET architecture, in the following research to solve this issue. The feature maps transmitted via skip connections include a lot of information detail, enabling deconvolution to recover a better image version.

ACKNOWLEDGEMENT

We want to acknowledge the climate modeling groups coordinated in SubX Projects (NASA, NOAA/NCEP, University of Miami, NRL, and Environment Canada) for developing and making their model output public. Also, we want to thank Agency for Meteorology Climatology and Geophysics (BMKG) for providing the ground observation dataset used in this study.

REFERENCES

Babaousmail H, Hou R, Gnitou GT, Ayugi B. 2021. Novel statistical downscaling emulator for precipitation projections using deep Convolutional Autoencoder over Northern Africa. *J Atmos Solar-Terrestrial Phys.* 218:1–11.

- Baker SA, Wood AW, Rajagopalan B. 2020. Application of postprocessing to watershed-scale subseasonal climate forecasts over the contiguous united states. *J Hydrometeorol.* 21(5):971–987.
- Baño-Medina J, Manzananas R, Gutierrez JM. 2020. Configuration and intercomparison of deep learning neural models for statistical downscaling. *Geosci Model Dev.* 13(4):2109–2124.
- Barker TW. 1991. The Relationship between spread and forecast error in extended-range forecasts. *J Clim.* 4(7):733–742.
- Funk C, Peterson P, Landsfeld M, Pedreros D, Verdin J, Shukla S, Husak G, Rowland J, Harrison L, Hoell A, *et al.* 2015. The climate hazards infrared precipitation with stations - a new environmental record for monitoring extremes. *Sci Data.* 2:1–21.
- Han L, Chen M, Chen K, Chen H, Zhang Y, Lu B, Song L, Qin R. 2021. A deep learning method for bias correction of ECMWF 24–240 h forecasts. *Adv Atmos Sci.* 38(9):1444–1459.
- Kirtman BP, Pegion K, DelSole T, Tippett M, Robertson AW, Bell M, Burgman R, Lin H, Gottschalck J, Collins DC, *et al.* 2017. *The subseasonal experiment (SUBX): IRI Data Libr.* [Accessed 2022 Jan 12]. <http://iridl.ldeo.columbia.edu/SOURCES/.Models/.SubX/>.
- Kolachian R, Saghafian B. 2019. Deterministic and probabilistic evaluation of raw and post-processed sub-seasonal to seasonal precipitation forecasts in different precipitation regimes. *Theor Appl Climatol.* 137(1–2):1479–1493.
- Krasnopolsky VM, Lin Y. 2012. A neural network nonlinear multimodel ensemble to improve precipitation forecasts over continental US. *Adv In Meteorol.* 2012:1–11.
- Kurniawan I, Silaban LS, Munandar D. 2020. Implementation of Convolutional Neural Network and Multilayer Perceptron in Predicting Air Temperature in Padang. *J RESTI (Rekayasa Sist dan Teknol Informasi).* 4(6):2–7.
- Le XH, Lee G, Jung K, An HU, Lee S, Jung Y. 2020. Application of convolutional neural network for spatiotemporal bias correction of daily satellite-based precipitation. *Remote Sens.* 12(2731):1–23.
- Li W, Chen J, Li L, Chen H, Liu B, Xu C-Y, Li X. 2019. Evaluation and bias correction of S2S precipitation for hydrological extremes. *J Hydrometeorol.* 20(9):1887–1906.
- Mao X-J, Shen C, Yang Y-B. 2016. *Image Restoration Using Convolutional Auto-encoders with Symmetric Skip Connections.* [Accessed 2022 Jan 12]. <http://arxiv.org/abs/1606.08921>.
- Misnawati, Boer R, June T, Faqih A. 2018. Perbandingan metodologi koreksi bias data curah hujan CHIRPS. *LIMNOTEK Perairan Darat Tropis di Indonesia.* 25(1):18–29.
- Monier E, Gao X, Scott JR, Sokolov AP, Schlosser CA. 2015. A framework for modeling uncertainty in regional climate change. *Clim Change.* 131(1):51–66.
- Muharsyah R, Hadi TW, Indratno SW. 2020. Penerapan metode Bayesian Model averaging untuk kalibrasi prediksi ensemble curah hujan bulanan di Pulau Jawa. *Agromet.* 34(1):20–33.
- Nover DM, Witt JW, Butcher JB, Johnson TE, Weaver CP. 2016. The effects of downscaling method on the variability of simulated watershed response to climate change in five U.S basins. *Earth Interact.* 20(11):1–27.
- Pegion K, Kirtman BP, Becker E, Collins DC, Lajoie E, Burgman R, Bell R, Delsole T, Min D, Zhu Y, *et al.* 2019. The subseasonal experiment (SUBX). *Bull Am Meteorol Soc.* 100(10):2043–2060.
- Ratri DN, Whan K, Schmeits M. 2019. A comparative verification of raw and bias-corrected ECMWF seasonal ensemble precipitation reforecasts in Java (Indonesia). *J Appl Meteorol Climatol.* 58(8):1709–1723.
- Robertson AW, Kumar A, Peña M, Vitart F. 2015. Improving and promoting subseasonal to seasonal prediction. *Bull Am Meteorol Soc.* 96(3):ES49–ES53.
- Robertson AW, Vitart F. 2019. *Sub-seasonal to Seasonal Prediction: The Gap Between Weather and Climate Forecasting.* 1st ed. Oxford: Elsevier Inc.

- Sandu I, Niekerk AV, Shepherd TG, Vosper SB, Zadra A, Bacmeister J, Beljaars A, Brown AR, Dörnbrack A, McFarlane N, *et al.* 2019. Impacts of orography on large-scale atmospheric circulation. *Nature Partner Journals: Clim Atmos Sci.* 2(1):1–8. doi:<http://dx.doi.org/10.1038/s41612-019-0065-9>.
- Vitart F, Ardilouze C, Bonet A, Brookshaw A, Chen M, Codorean C, Déqué M, Ferranti L, Fucile E, Fuentes M, *et al.* 2017. The subseasonal to seasonal (S2S) prediction project database. *Bull Am Meteorol Soc.* 98(1):163–173.
- Vuillaume JF, Dorji S, Komolafe A, Herath S. 2018. Sub-seasonal extreme rainfall prediction in the Kelani River basin of Sri Lanka by using self-organizing map classification. *Nat Hazards.* 94(1):385–404. doi:<https://doi.org/10.1007/s11069-018-3394-9>.
- Wang C, Jia Z, Yin Z, Liu F, Lu G, Zheng J. 2021. Improving the accuracy of subseasonal forecasting of china precipitation with a machine learning approach. *Front Earth Sci.* 9:1–9.
- White CJ, Carlsen H, Robertson AW, Klein RJT, Lazo JK, Kumar A, Vitart F, Perez ECD, Ray AJ, Murray V, *et al.* 2017. Potential applications of subseasonal-to-seasonal (S2S) predictions. *Meteorol Appl.* 24(3):315–325.